R. & M. No. 3116
(20,010)
A.R.C. Technical Report

MINISTRY OF SUPPLY

AERONAUTICAL RESEARCH COUNCIL
REPORTS AND MEMORANDA

A Theory of the Separated Flow from the Curved Leading Edge of a Slender Wing

By
J. H. B. SMITH

LONDON : HER MAJESTY'S STATIONERY OFFICE
1959
PRICE 6*s*. 6*d*. NET

A Theory of the Separated Flow from the Curved Leading Edge of a Slender Wing

By

J. H. B. Smith

Communicated by the Director-General of Scientific Research (Air), Ministry of Supply

Reports and Memoranda No. 3116*

November, 1957

Summary.—The simple model used by Brown and Michael to represent the flow past a slender delta wing with leading edge separation, is extended to treat wings which have pointed apexes, curved leading edges and straight, unswept trailing edges. The vorticity of the fluid near the leading edge is represented by an isolated vortex of varying strength, which is curved in the non-conical cases considered here. A step-by-step method of calculation is used which starts from an assumed conical flow near the apex and employs the condition of zero total force on the vortex system in one cross-flow plane to obtain the configuration in the next. Numerical values of the co-ordinates and strength of the vortex, the lift coefficient and the centre-of-pressure position are found for three plan-form families at different incidences.

1. *Introduction.*—The flow past a highly swept leading edge usually separates there, with the formation of a core of rotating fluid above and inboard of the leading edge, joined to it by a vortex layer. Potential-flow models representing this type of flow with separation from all edges of a wing have been proposed by several authors (Legendre[1], Brown and Michael[2], Mangler and Smith[3, 4], Küchemann[5], Roy[6]), for the flat plate delta wing, on the assumption of conical flow. In Ref. 3, it is supposed that the vorticity of the fluid is concentrated into vortex sheets springing from the leading edges and rolling up into spirals in the core regions. The shapes of these and the distribution of vortex strength along them are determined in principle by the two boundary conditions that a vortex sheet must lie in a stream surface and that it cannot sustain a pressure difference. Calculations based on this model, employing slender-wing theory, are described in Ref. 4.

If this model is simplified by condensing the entire vorticity of the sheets into a pair of isolated vortices, joined to the leading edges by cuts†, it is found that a pressure difference remains across the cuts. This is an unrealistic feature of the model, which arises from the simplifications introduced. However, the force acting on the cut can be balanced by the force which acts on the isolated vortex terminating it owing to the vortex not lying along a streamline. The pressure difference across the cut is constant, and so the force on it is independent of its shape between the lines that bound it, *viz.*, the isolated vortex and the leading edge. When the condition of zero total force on cut and vortex combined is applied, together with the condition of finite velocity at the wing leading edge (smooth outflow condition), we obtain the model studied by Brown and Michael[2].

* R.A.E. Tech. Note Aero. 2535, received 24th March, 1958.

† These are curves across which a jump in the potential occurs. They are a feature of the mathematical model only, required to keep the velocity potential single valued.

Here, this treatment is applied to the flow separated from the leading edge of a flat slender wing of more general plan-form. The only restrictions on the plan-form are to pointed noses, unswept trailing edges, and leading edges without discontinuities of slope. The conditions in each cross-flow plane, which now involve the variation in the streamwise direction of the strength and relative position of the vortex, are no longer sufficient to determine the solution. However, if the strength and position of the vortex are known at one streamwise station, these values can be used to calculate their rates of change there and thus the strength and position may be found at a neighbouring station downstream. In the neighbourhood of the pointed apex of the wing, the conical solution of Ref. 2 may be introduced to initiate the procedure. Thus a step-by-step method is obtained by which this model of the flow can be calculated. The step size is regulated by the rate of change of the leading-edge slope : if the slope changes too much from one step to the next, large changes in vortex position and strength are predicted and these seem to be over-corrected at the following step, leading to a divergent oscillation in the numerical solution. Thus a discontinuity in leading-edge slope can only be treated by fairing it with a smooth curve and using an appropriately small step size.

The properties of several families of plan-forms at different incidences have been calculated, more as test cases than as part of a systematic investigation. The results obtained are interpreted by making use of the relations between the delta-wing solutions of Ref. 2, where the present model is used, and those of Ref. 4, where a more elaborate model is used.

2. *Method of Calculation.*—We consider the configuration shown in Fig. 1. With axes fixed in the wing, origin at the apex, Ox along the centre-line, Oy to starboard, Oz upwards, the free stream is at an incidence α to Ox. We resolve it, for small incidences, into U along Ox and αU along Oz. We shall make use of the complex co-ordinate $Z = y + iz$ in the plane $x =$ constant, known as the cross-flow plane.

The separated flow is represented in the first place by vortex sheets springing from the leading edges and rolling up into spirals, this configuration being determined in principle by the two conditions that the sheets lie in stream surfaces and sustain no pressure difference. This model is then simplified by condensing the vorticity of each sheet into an isolated vortex, leaving the trace of the sheet as a cut, across which the velocity potential is discontinuous. A pressure difference now remains across the cut, so long as the isolated vortex continues to grow in strength in the streamwise direction. Since the cross-flow velocities (in the plane $x =$ constant) are continuous across the cut now that the vorticity has been condensed, we can write this pressure difference, ΔC_p, by slender-wing theory, as

$$\Delta C_p = -\frac{2}{U}\Delta\Phi_x = -\frac{2}{U}\frac{d\Gamma}{dx}, \qquad \ldots\ldots\ldots\ldots\ldots \quad (1)$$

for the right-hand vortex, where Δ means the difference taken 'inside' minus 'outside', Φ is the velocity potential and Γ the strength of the isolated vortex.

This pressure difference is a function of x only, so that the force acting in the plane $x = x_0$ on a section of the cut lying between the planes $x = x_0$ and $x = x_0 + \delta x$ is given at once as

$$-i(Z_0 - s)\tfrac{1}{2}\rho U^2 \Delta C_p \, \delta x \,,$$

where $Z_0 = y_0 + iz_0$ is the point where the right-hand isolated vortex meets the plane $x = x_0$ and s is the local semi-span of the wing in this plane. Thus, using equation (1), the force on this section of the cut is

$$i\rho U \, \delta x \, (Z_0 - s)\frac{d\Gamma}{dx}. \qquad \ldots\ldots\ldots\ldots\ldots \quad (2)$$

This force is to be balanced by an equal and opposite force acting in the plane $x = x_0$ on the section of the right-hand isolated vortex between the planes $x = x_0$ and $x = x_0 + \delta x$. By the well-known formula this is the product of $-i\rho\Gamma \, \delta x$ and the velocity normal to the isolated

vortex at its station due to the remainder of the flow field. This velocity is due in part to the components v_1 and w_1 of the cross-flow at the station of the isolated vortex due to the remainder of the cross-flow field and in part to the free-stream component normal to the vortex (the perturbation velocity parallel to Ox makes a contribution of higher order). The free-stream component normal to the vortex has components $-U(dy_0/dx)$ and $-U(dz_0/dx)$ parallel to Oy and Oz, where the co-ordinates of the vortex are regarded as functions of x. Thus the force on the section of the isolated vortex is

$$-i\rho\Gamma\,\delta x\left\{v_1 - U\frac{dy_0}{dx} + i\left(w_1 - U\frac{dz_0}{dx}\right)\right\}. \qquad \ldots \qquad \ldots \qquad \ldots \qquad (3)$$

Equating the sum of (2) and (3) to zero and re-arranging, we find

$$\frac{\Gamma}{U}(v_1 + iw_1) = (Z_0 - s)\frac{d\Gamma}{dx} + \Gamma\frac{dZ_0}{dx}. \qquad \ldots \qquad \ldots \qquad \ldots \qquad \ldots \qquad (4)$$

The two-dimensional potential in the cross-flow plane must have the following properties. At infinity, the velocity w parallel to Oz must tend to αU. On the wing, the normal velocity must vanish. At the leading edge the velocity must be finite, *i.e.*, the outflow is smooth. In the neighbourhood of $Z = Z_0$ and $-\bar{Z}_0$, the potential must have the singularities associated with vortices of strengths $\pm\Gamma$. The complex potential, W, is most easily constructed in the plane Z^*, where

$$Z^{*2} = Z^2 - s^2. \qquad \ldots \qquad \ldots \qquad \ldots \qquad \ldots \qquad \ldots \qquad \ldots \qquad (5)$$

Under this transformation, the wing slit (Z real, $|Z| \leqslant s$) becomes part of the imaginary axis and is a streamline by symmetry. Conditions at infinity are unchanged, but the point $Z^* = 0$, $Z = \pm s$ is singular, so that a finite velocity at the leading edge in the cross-flow plane arises from a stagnation point in the transformed plane. Thus for the complex potential we have :

$$W = -i\alpha UZ^* + \frac{\Gamma}{2\pi i}\log\frac{Z^* - Z_0^*}{Z^* + \bar{Z}_0^*}, \qquad \ldots \qquad \ldots \qquad \ldots \qquad (6)$$

where $Z^* = Z_0^*$ is the point corresponding to $Z = Z_0$, the position of the right-hand vortex. The smooth outflow condition is expressed by $dW/dZ^* = 0$ for $Z^* = 0$, i.e.,

$$\frac{\Gamma}{2\pi\alpha U} = \frac{Z_0^*\,\bar{Z}_0^*}{Z_0^* + \bar{Z}_0^*}. \qquad \ldots \qquad \ldots \qquad \ldots \qquad \ldots \qquad \ldots \qquad \ldots \qquad (7)$$

The conjugate of the velocity $v_1 + iw_1$ due to the remainder of the flow field at the station of the right-hand vortex is given by

$$v_1 - iw_1 = \left.\frac{dW_1}{dZ}\right|_{Z=Z_0},$$

where

$$W_1 = W - \frac{\Gamma}{2\pi i}\log(Z - Z_0).$$

After some manipulation, using equations (5), (6) and (7), we find

$$v_1 - iw_1 = \frac{\Gamma}{2\pi i}\frac{Z_0}{Z_0^*}\left(\frac{Z_0^* + \bar{Z}_0^*}{Z_0^*\,\bar{Z}_0^*} - \frac{1}{Z_0^* + \bar{Z}_0^*} - \frac{s^2}{2Z_0^{\,2}\,Z_0^*}\right).$$

Combining this with the conjugate of (4) yields

$$\frac{U}{\Gamma}\left((\bar{Z}_0 - s)\frac{d\Gamma}{dx} + \Gamma\frac{d\bar{Z}_0}{dx}\right) = \frac{\Gamma}{2\pi i}\frac{Z_0}{Z_0^*}\left(\frac{Z_0^* + \bar{Z}_0^*}{Z_0^*\,\bar{Z}_0^*} - \frac{1}{Z_0^* + \bar{Z}_0^*} - \frac{s^2}{2Z_0^{\,2}\,Z_0^*}\right). \qquad \ldots \qquad (8)$$

Equations (7) and (8), equivalent to three real equations, together with appropriate initial values at some station $x =$ constant, determine the solution. In the case of the conical flow past a delta wing, Γ and Z_0 are known to be proportional to x and the equations reduce to the

algebraic equations solved by Brown and Michael[2]. In the present case, we assume that in the neighbourhood of the apex of the wing (supposed pointed), the flow is approximately conical. We use (7) to eliminate Γ and its derivative from (8). The real and imaginary parts of the resulting equation are then simultaneous ordinary linear first-order differential equations for y_0 and z_0, which can be solved by step-by-step integration for a given plan-form (*i.e.*, given $s = s(x)$) and incidence, using the boundary values obtained from the assumed conical flow near $x = 0$.

In practice non-dimensional quantities have been used and the equations simplified as described in Appendix I. Equations (I.7) and (I.8) provide a routine which leads from the co-ordinates and strength of the vortex at $x = x_0$ to those at $x = x_0 + \Delta x$ for a particular plan-form and incidence. The time taken for each step was about 30 minutes on a fully automatic desk machine. No general rule about the size of step, Δx, can be given. It must be small when the slope of the leading edge changes rapidly and also when the local semi-span is small. It can apparently be larger for a higher incidence on the same plan-form, without leading to a divergent oscillation in the results. Tables 1 to 3 show the actual step sizes used in the calculation carried out, but no systematic attempt was made to enlarge the step size or to try the effect on the results of reducing it.

The co-ordinates and strength of the isolated vortex in the cross-flow plane $x = c$ lead directly to the lift acting on that part of the plan-form forward of $x = c$. Denoting this by $L(c)$, we have, by considering the momentum integral (*cf.*, equation (18) of Ref. 2),

$$L(c) = \rho U^2(\pi\alpha + 2\gamma\sigma)s^2(c) , \quad .. \quad .. \quad .. \quad .. \quad .. \quad (9)$$

where $s(c)$ is the semi-span at $x = c$, and γ and σ are the non-dimensional vortex strength and a non-dimensional co-ordinate introduced in Appendix I ($2\sigma s$ is the distance separating the vortices in the transformed plane). Thus the lift coefficient is given by

$$C_L = \tfrac{1}{2}A(\pi\alpha + 2\gamma\sigma) . \quad .. \quad .. \quad .. \quad .. \quad .. \quad (10)$$

The centre of pressure of the wing terminated by a straight unswept trailing edge at $x = c$ is at the point

$$x = hc = \frac{\int_0^c x \frac{dL}{dx}\, dx}{L(c)} = \frac{cL(c) - \int_0^c L(x)\, dx}{L(c)} .$$

Thus the distance of the centre of pressure from the apex is a fraction h of the chord where

$$h = 1 - \frac{\int_0^c L(x)\, dx}{cL(c)} . \quad .. \quad .. \quad .. \quad .. \quad .. \quad (11)$$

Since, in slender-wing theory, the flow upstream of the plane $x = c$ is unaffected by changes downstream of it, it is natural to consider each step of the step-by-step integration as terminating a plan-form with a straight trailing edge. Thus the solution for a particular plan-form at a certain incidence includes the solutions for a family of plan-forms at this incidence, obtained by cutting it short at different chordwise stations.

The basic plan-forms considered are shown in Figs. 2, 3 and 4. The cropped delta (apex angle 90 deg) with slight fairing of Fig. 2 was calculated at an incidence of $0{\cdot}4$ radian ($= 22{\cdot}9$ deg) only. The results for various chord lengths are given in Table 1. Tabulated are the non-dimensional (η, ζ) and dimensional (y_0, z_0) co-ordinates of the isolated vortex ($y_0 = \eta s$, $z_0 = \zeta s$) ; the vortex strength (Γ/U) ; the lift coefficient C_L ; the distance, h, in chord lengths, of the centre of pressure from the apex ; the local aspect ratio, local semi-span and cotangent of local sweep (A, s and s') ; and the values of lift coefficient and centre of pressure position ($C_{L\,\mathrm{Att}}$ and h_{Att}) calculated on the basis of attached-flow theory. In Tables 2 and 3 the same quantities are listed

for the fully-faired cropped delta (apex angle 28 deg.) of Fig. 3 at $\alpha = 5{\cdot}73$ deg ($0{\cdot}1^c$) and $11{\cdot}45$ deg ($0{\cdot}2^c$) and the extended 'Gothic' wing of Fig. 4 at $\alpha = 15{\cdot}3$ deg and $30{\cdot}6$ deg. The numbers tabulated are quoted to more significant figures than is justified by the simple technique used to solve equations (7) and (8), in order to illustrate the behaviour of the process. The projections of the vortex paths on to the co-ordinate planes are shown in Figs. 2, 3, and 4 for the larger incidences. Fig. 5 shows the non-dimensional height of the vortex above the trailing edge of a number of members of the plan-form families calculated, plotted against the ratio of incidence to aspect ratio. In Fig. 6 the lift coefficient divided by αA is plotted against α/A for the same wings.

3. *Discussion of Results.*—The results calculated for the position of the isolated vortex are listed in columns 4 to 7 of Tables 1 to 3. In addition, the three projections of the vortex on to the co-ordinate planes are drawn in Figs. 2 to 4 for one incidence in each case. We see that, on these convex plan-forms, the vortex approaches the leading edge in plan view as we go downstream, crosses it and then continues to move slowly outboard. Owing to the increasing local sweep-back angle, however, the inclination of the plan projection of the vortex to the centre-line decreases. On the other hand, the vortex not only continues to rise above the wing as we go downstream, but also its inclination to the plane of the wing increases, to become of the order of one half the incidence. This is of interest in that the streamwise parts of the leading edges of these plan-forms can be regarded as side edges. The upper edge of the vortex sheet from the side edge of a retangular plan-form has been taken to be inclined at $\alpha/2$ to the wing and the stream by Mangler[7], following a suggestion of Betz. Regarding the calculations as applying to families of plan-forms obtained by terminating the basic plan-forms (Figs. 2 to 4) at different chordwise stations, we can consider the height of the vortex above the wing trailing edge for a variety of wings and incidences. In Fig. 5 the height, made non-dimensional by reference to the span, is plotted against the ratio of incidence to aspect ratio. For delta wings, the same mathematical model of the flow was calculated by Brown and Michael[2] and their curve is also shown in Fig. 5. The scatter of the points is small enough for it to be guessed that the non-dimensional height is a function of α/A only, in a first approximation. If this is so in this mathematical model, it may well be so in others and also in real flows where trailing-edge effects are small. There is, therefore, some reason to think that the second curve in Fig. 5 drawn from Ref. 4, where a more sophisticated model was studied for the delta wing, may be a better guide to the relationship between the non-dimensional vortex height, ζ, and α/A. However, some caution is needed in predicting details of real flows from the mathematical models. Experimental results for the vortex positions on the delta wing at low speeds are not yet in agreement with each other and differ in almost all cases from those calculated in Ref. 4. In spite of this, the theoretical results of Ref. 4 are preferred to those of Ref. 2 ; furthermore, these difficulties do not affect the conjecture that the non-dimensional height depends primarily on α/A.

The lift coefficients of the members of the plan-form families are listed in column 9 of Tables 1 to 3, with their aspect ratios and their lift coefficients as calculated by R. T. Jones's slender-wing theory for attached flow in columns 11 and 12 for comparison. Although the lift coefficient still falls as the wing is extended downstream with increasing sweep, the fall with aspect ratio is much slower than in the attached-flow theory. This is because R. T. Jones's theory predicts no lift on any part of a flat wing where the local span is constant, while the present model predicts lift forces due to changes in the vortex strength and position. In Fig. 6 the lift coefficients, divided in each case by the product αA, are plotted against α/A, the parameter used to collapse the vortex heights. R. T. Jones's theory yields the horizontal line shown. The values for the present curved-edge plan-forms lie reasonably close to the curve for the delta plan-form, drawn from Ref. 2. We may guess therefore, that calculations using other models would show the same behaviour, *viz.*,

$$C_L \simeq \alpha A f(\alpha/A) , \qquad \ldots\ldots\ldots\ldots\ldots\ldots \quad (12)$$

where f depends on the mathematical model, but not the plan-form. Now the function f was found for delta wings in Ref. 4 by calculating a more sophisticated model, so the curve drawn

from Ref. 4 in Fig. 6 may be taken as the best theoretical estimate available for the lift coefficient of wings with this type of flow, regardless of leading-edge shape. A simple expression was found in Ref. 4 to fit f closely ; it now becomes :

$$\left.\begin{array}{ll} C_L = \frac{\pi}{2}\alpha A\left(1+\frac{8}{\pi}\left|\frac{\alpha}{A}\right|\right) & |\alpha| \leqslant 0{\cdot}4A \\ \text{or} & \\ C_L = C_{L\,\text{Att}} + 4\alpha^2 & 0 \leqslant \alpha \leqslant 0{\cdot}4A \end{array}\right\} \quad \ldots \quad \ldots \quad \ldots \quad (13)$$

The centre-of-pressure position is given as a fraction of the chord in column 10 of the Tables with the value on R. T. Jones's theory of attached flow in column 13 for comparison. Except for the delta wings, where the flow on both theories is conical, the present theory predicts a centre-of-pressure position nearer the trailing edge, the difference becoming large as the plan-form deviates more from the delta. There is also a change of centre of pressure with incidence ; the movement being backward as the incidence increases, on a particular plan-form. However, plan-forms of this type can still yield centres of pressure well forward of the 2/3 chord point found for the delta.

With certain exceptions, the strength of the isolated vortex (column 8 of the Tables), increases in the streamwise direction, though the rate of growth becomes much less as the leading edge inclines towards the streamwise direction. At first sight it appears impossible for the strength to decrease, since this would imply the shedding of negative vorticity from the leading edge. The fact that such a decrease is found in the calculations for the lower incidences and the more sharply curved leading edges (Table 1, $1{\cdot}25 \leqslant x \leqslant 1{\cdot}60$; Table 2 (a), $1{\cdot}8 \leqslant x \leqslant 2{\cdot}2$), would then indicate a defect in the mathematical model or in the calculation. However, in Fig. 7 are plotted the bound vortex configurations on a delta wing at two different incidences, calculated for the model of Ref. 4. From this it is clear that if the plan-forms could be cropped along the dashed lines without altering the bound vortex configurations, negative vorticity would be shed from the part a–a of the leading (tip) edge at the lower incidence. At the higher incidence the vorticity shed from the leading (tip) edge would be positive. The values of α/A for the delta wings of Fig. 7 correspond roughly to those of the member of plan-form family II terminating in the region of decreasing vortex strength, at the two calculated incidences. Since, at the higher incidence, this decrease is not found in the calculation and no decrease is found on the smoother plan-form of Fig. 4, we may suppose that this decrease, when it occurs, is neither a consequence of the calculation method nor of the simplification of the model from that of Ref. 4. This still does not imply that it would be found experimentally, since slender-wing theory itself may be inadequate to treat wings with sharply curved leading edges.

When comparing the results discussed above with experiment, or using them to predict the characteristics of aircraft designs, the following features of the model must be borne in mind :

(a) No account is taken of trailing-edge effects. At subsonic speeds these may be large and may be expected to produce loss of lift on the rear part of the plan-form and movement of the vortices closer to the stream direction. Thus the overall lift coefficient will be reduced and the centre of pressure moved forward. The effects will be greatest on those plan-forms where theory predicts the highest loads near the trailing edge, *i.e.*, the deltas, and lower on plan-forms with substantial regions of constant span. At supersonic speeds the effect of the trailing edge is likely to be much less.

(b) No account is taken of secondary separation of the boundary layer in the adverse pressure gradient between the projection of the vortex and the leading edge. This will certainly tend to spread and reduce the suction peaks predicted, but need have little effect on the lift. Its influence on the vortex position is unknown, but may be considerable.

(*c*) No account is taken of wing thickness. The effect of this on the distribution of lifting pressure is unknown. It was shown in Ref. 4 that, if the lifting pressure distribution on a delta wing was unaffected by the presence of a symmetrical thickness distribution, the lift-dependent drag was reduced by a term proportional to the thickness/chord ratio. Since, for large values of the thickness/chord ratio, this implies the absurdity of negative lift-dependent drag, we must conclude that the lifting pressures are modified on thick wings.

(*d*) No account is taken of compressibility. For attached flow, the slender-wing theory can be compared at many points with supersonic linearised theory; no theoretical studies of leading-edge separation capable of indicating the variation of the flow field with Mach number are known. It is also possible that, at high speeds and incidences, a shock may occur in the fluid between the vortices, in which case the present treatment is inadequate.

4. *Conclusions.*—A method has been given for calculating a simplified model of the flow past a thin, slender, pointed wing, with unswept trailing edge, which takes account of the separation of the flow at the leading edge. Numerical results calculated suggest that the relations giving the height of the vortex above the wing and the lift coefficient in terms of the ratio of incidence to aspect ratio for the delta wing apply to more general convex plan-forms. Although the limitations of the model have to be remembered in applying the results to real flows, the treatment should be adequate to show the variations in aerodynamic characteristics occurring with separation and also to indicate the effect of plan-form variation on these characteristics in separated flow.

LIST OF SYMBOLS

A		Aspect ratio
c		Root chord
C_L		Lift coefficient
$C_{L\,\mathrm{Att}}$		Lift coefficient on attached-flow theory
C_p		Pressure coefficient
h		Distance of centre of pressure from apex, referred to root chord
h_{Att}		The same on attached-flow theory
$L(x)$		Lift on plan-form terminated at x
$s(x)$		Local semi-span
U		Free-stream velocity
$v_1 + iw_1$		Cross-flow velocity at station of right-hand vortex due to remainder of flow field
W		Complex potential
x, y, z		Rectangular cartesian co-ordinates, origin at wing apex, Ox along centre-line downstream, Oy to starboard, Oz upwards.
Z	$=$	$y + iz$ (complex co-ordinate in cross-flow plane)
Z_0	$=$	$y_0 + iz_0$ (position of right-hand vortex)
Z^*	$=$	$(Z^2 - s^2)^{1/2}$ (complex co-ordinate in transformed plane)
α		Incidence
Γ		Strength of right-hand vortex
γ	$=$	Γ/Us
Δ		Difference operator across vortex sheet or cut : 'inside' — 'outside'
$\eta + i\zeta$	$=$	Z_0/s
Φ		Perturbation potential
ρ		Density
$\sigma + i\tau$	$=$	$Z_0{}^*s$

REFERENCES

No.	*Author*	*Title, etc.*
1	R. Legendre	Ecoulement au voisinage de la pointe avant d'une aile à forte flèche aux incidences moyennes. *La Recherche Aéronautique* (O.N.E.R.A.), No. 31, 1953. Translated as A.R.C. 16796. Presented at the 8th International Congress on Theoretical and Applied Mechanics. August, 1952.
2	C. E. Brown and W. H. Michael ..	On slender delta wings with leading edge separation. N.A.C.A. Tech. Note 3430. April, 1955. Published in *J. Ae. Sci.*, Vol. 21, p. 690. October, 1954.
3	K. W. Mangler and J. H. B. Smith	A theory of slender delta wings with leading-edge separation. R.A.E. Tech. Note Aero. 2442. A.R.C. 18,757. April, 1956.
4	K. W. Mangler and J. H. B. Smith	Calculation of the flow past slender delta wings with leading-edge separation. R.A.E. Report Aero. 2593. A.R.C. 19,634. May, 1957.
5	D. Küchemann	A non-linear lifting-surface theory for wings of small aspect ratio with edge separations. R.A.E. Report Aero. 2540. A.R.C. 17,769. April, 1955.
6	M. Roy	Sur la théorie de l'aile en delta.—Tourbillons d'apex et nappes en cornet. *La Recherche Aéronautique* (O.N.E.R.A.) No. 56. February, 1957.
7	K. W. Mangler	Der kleinste induzierte Widerstand eines Tragflügels mit kleinem Seitenverhältnis. Jahrbuch 1939 der deutschen Luftfahrtforschung, Pt. I, p. 139.

APPENDIX I

Reduction of the Equations to a Form Amenable to Numerical Calculation

We make the substitutions :

$$\Gamma = \gamma U s\,, \qquad Z_0 = (\eta + i\zeta)s\,, \qquad Z_0{}^* = (\sigma + i\tau)s$$

in equations (5), (7) and (8) of Section 2. We obtain :

from (5) :

$$\sigma^2 - \tau^2 + 2i\sigma\tau = \eta^2 - \zeta^2 - 1 + 2i\eta\zeta \quad .. \quad .. \quad .. \quad .. \quad .. \quad \text{(I.1)}$$

from (7) :

$$\frac{\gamma}{2\pi\alpha} = \frac{\sigma^2 + \tau^2}{2\sigma} \quad .. \quad .. \quad .. \quad .. \quad .. \quad .. \quad .. \quad \text{(I.2)}$$

from (8)

$$s(\eta' - i\zeta') + s'(2\eta - 1 - 2i\zeta) + s\frac{\gamma'}{\gamma}(\eta - 1 - i\zeta)$$

$$= \frac{i\gamma}{2\pi}\left\{\frac{(\eta - i\zeta)(\sigma - i\tau)^2}{2(\eta^2 + \zeta^2)(\sigma^2 + \tau^2)^2} + \frac{(\eta + i\zeta)(\sigma - i\tau)}{\sigma^2 + \tau^2}\left(\frac{1}{2\sigma} - \frac{2\sigma}{\sigma^2 + \tau^2}\right)\right\}, \quad .. \quad .. \quad \text{(I.3)}$$

where the prime denotes differentiation with respect to x. Now the real and imaginary parts of (I.3) can be written, using (I.2) for γ, as

$$\left.\begin{aligned} s\eta' &= A\alpha - s'(2\eta - 1) + s(1 - \eta)\frac{\gamma'}{\gamma} \\ \text{and} \qquad & \\ s\zeta' &= B\alpha - 2\zeta s' - s\zeta\frac{\gamma'}{\gamma} \end{aligned}\right\}, \quad .. \quad .. \quad .. \quad .. \quad \text{(I.4)}$$

where A and B are listed below. By differentiating (I.1), separating real and imaginary parts and solving we have :

$$\left.\begin{aligned} \sigma'(\sigma^2 + \tau^2) &= \eta'(\sigma\eta + \tau\zeta) + \zeta'(\tau\eta - \sigma\zeta) \\ \tau'(\sigma^2 + \tau^2) &= \eta'(\sigma\zeta - \tau\eta) + \zeta'(\tau\zeta + \sigma\eta) \end{aligned}\right\}. \quad .. \quad .. \quad .. \quad .. \quad .. \quad \text{(I.5)}$$

Differentiating (I.2) logarithmically yields :

$$\begin{aligned} \frac{\gamma'}{\gamma} &= \frac{(\sigma^2 - \tau^2)\sigma' + 2\sigma\tau\tau'}{\sigma(\sigma^2 + \tau^2)} \\ &= -C\eta' - D\zeta' \quad .. \quad .. \quad .. \quad .. \quad .. \quad .. \quad .. \quad \text{(I.6)} \end{aligned}$$

by (I.5), where C and D are listed below. The three equations (I.4) to (I.6) are now solved, by substituting in (I.6) for η' and ζ' to give

$$\frac{\gamma'}{\gamma} = \frac{\{s'(2\eta - 1) - A\alpha\}C + (2\zeta s' - B\alpha)D}{s\{1 + (1 - \eta)C - \zeta D\}}$$

and hence, by (I.4)

$$\eta' = \frac{A\alpha}{s} - \frac{s'}{s}(2\eta - 1) + \frac{1 - \eta}{s\{1 + (1 - \eta)C - \zeta D\}}\left[\{s'(2\eta - 1) - A\alpha\}C + (2\zeta s' - B\alpha)D\right]$$

$$\zeta' = \frac{B\alpha}{s} - \frac{s'}{s}2\zeta - \frac{\zeta}{s\{1 + (1 - \eta)C - \zeta D\}}\left[\{s'(2\eta - 1) - A\alpha\}C + (2\zeta s' - B\alpha)D\right], \quad .. \quad \text{(I.7)}$$

where

$$A = \frac{1}{2\sigma(\sigma^2+\tau^2)}\left[\frac{\zeta\{\eta^2 - \frac{1}{2}(\tau^2-\sigma^2)\}}{\eta^2+\zeta^2} + \frac{(\eta\tau - \zeta\sigma)(\tau^2-3\sigma^2)}{2\sigma}\right]$$

$$B = \frac{1}{2\sigma(\sigma^2+\tau^2)}\left[\frac{\eta\{\zeta^2 + \frac{1}{2}(\tau^2-\sigma^2)\}}{\eta^2+\zeta^2} - \frac{(\eta\sigma + \zeta\tau)(\tau^2-3\sigma^2)}{2\sigma}\right]$$

$$C = \frac{\tau^2(3\eta\sigma + \zeta\tau) - \sigma^2(3\zeta\tau + \eta\sigma)}{\sigma(\sigma^2+\tau^2)^2}$$

$$D = \frac{\tau^2(\eta\tau - 3\zeta\sigma) - \sigma^2(3\eta\tau - \zeta\sigma)}{\sigma(\sigma^2+\tau^2)^2} \qquad \text{(I.8)}$$

TABLE 1

Solutions for the Family of Plan-forms I, Fig. 2, at Incidence 22·9° = 0·4^c

c	s	s'	η	ζ	y_0	z_0	Γ/U	C_L	h	A	$C_{L\,\mathrm{Att}}$	h_{Att}
1	1	1	0·9110	0·0975	0·9110	0·0975	1·661	3·78	0·667	4	2·51	0·667
1·025	1·024	0·95	0·9110	0·0974	0·9329	0·0997	1·701					
1·050	1·048	0·90	0·9115	0·0983	0·9552	0·1030	1·729					
1·075	1·069	0·85	0·9122	0·0997	0·9751	0·1066	1·747					
1·100	1·090	0·80	0·9130	0·1019	0·9952	0·1111	1·759	3·74		3·930		
1·125	1·109	0·75	0·9137	0·1038	1·0133	0·1151	1·771					
1·150	1·128	0·70	0·9145	0·1060	1·0316	0·1196	1·782					
1·200	1·160	0·60	0·9162	0·1113	1·0628	0·1291	1·793	3·62		3·750		
1·250	1·188	0·50	0·9180	0·1175	1·0906	0·1396	1·801					
1·300	1·210	0·40	0·9204	0·1244	1·1137	0·1505	1·796	3·45		3·502		
1·350	1·228	0·30	0·9233	0·1322	1·1338	0·1623	1·786					
1·400	1·240	0·20	0·9270	0·1413	1·1495	0·1752	1·767	3·26		3·208		
1·450	1·248	0·10	0·9317	0·1519	1·1628	0·1896	1·748					
1·500	1·250	0	0·9376	0·1635	1·1720	0·2044	1·722	3·05	0·599	2·884	1·81	0·566
1·600	1·250	0	0·9527	0·1895	1·1909	0·2369	1·686	2·87		2·586		
1·700	1·250	0	0·9645	0·2110	1·2056	0·2638	1·691	2·72		2·344		
1·800	1·250	0	0·9732	0·2297	1·2165	0·2871	1·716	2·58		2·142		
1·900	1·250	0	0·9804	0·2471	1·2255	0·3089	1·749	2·47		1·973		
2·100	1·250	0	0·9928	0·2800	1·2410	0·3500	1·825	2·28	0·516	1·704	1·07	0·405
2·300	1·250	0	1·0027	0·3104	1·2534	0·3880	1·907	2·13		1·500		
2·500	1·250	0	1·0101	0·3394	1·2626	0·4243	1·990	2·01		1·340		
2·700	1·250	0	1·0169	0·3673	1·2711	0·4591	2·072	1·91		1·210		
2·900	1·250	0	1·0228	0·3943	1·2785	0·4929	2·154	1·82	0·465	1·103	0·69	0·293

TABLE 2 (*a*)

Solutions for the Family of Plan-forms II, Fig. 3, at Incidence 5·73° = 0·1^c

c	s	s'	η	ζ	y_0	z_0	Γ/U	C_L	h	A	$C_{L\,\mathrm{Att}}$	h_{Att}
1·0	0·2500	0·250	0·9100	0·1000	0·2275	0·0250	0·1041					
1·1	0·2750	0·250	0·9109	0·0979	0·2505	0·0269	0·1142	0·236	0·667	0·998	0·157	0·667
1·2	0·2988	0·225	0·9110	0·0975	0·2722	0·0291	0·1241					
1·3	0·3200	0·200	0·9141	0·1034	0·2927	0·0331	0·1276	0·231		0·970		
1·4	0·3388	0·175	0·9154	0·1084	0·3101	0·0367	0·1324					
1·5	0·3550	0·150	0·9159	0·1106	0·3252	0·0393	0·1377	0·218	0·642	0·906	0·142	0·636
1·6	0·3688	0·125	0·9195	0·1206	0·3391	0·0445	0·1378					
1·7	0·3800	0·100	0·9220	0·1301	0·3504	0·0494	0·1393	0·204		0·820		
1·8	0·3888	0·075	0·9250	0·1406	0·3596	0·0547	0·1423					
1·9	0·3950	0·050	0·9292	0·1535	0·3670	0·0606	0·1405	0·189	0·603	0·726	0·114	0·575
2·0	0·3988	0·025	0·9367	0·1667	0·3735	0·0665	0·1386					
2·1	0·4	0	0·9440	0·1822	0·3776	0·0729	0·1379	0·172		0·628		
2·2	0·4	0	0·9540	0·1960	0·3816	0·0784	0·1360					
2·3	0·4	0	0·9623	0·2121	0·3849	0·0848	0·1365	0·158	0·550	0·543	0·085	0·485
2·4	0·4	0	0·9693	0·2268	0·3877	0·0907	0·1379					
2·5	0·4	0	0·9754	0·2407	0·3902	0·0963	0·1397	0·147		0·478		
2·6	0·4	0	0·9807	0·2539	0·3923	0·1016	0·1419					
2·8	0·4	0	0·9902	0·2793	0·3961	0·1117	0·1465	0·135	0·510	0·406	0·064	0·398
3·0	0·4	0	0·9980	0·3033	0·3992	0·1213	0·1515	0·129		0·369		
3·2	0·4	0	1·0065	0·3251	0·4026	0·1300	0·1558	0·122	0·489	0·338	0·053	0·348

TABLE 2 (*b*)

Solutions for the Family of Plan-forms II, Fig. 3, at Incidence 11·45° = 0·2^c

c	s	s'	η	ζ	y_0	z_0	Γ/U	C_N	h	A	$C_{N\,\mathrm{Att}}$	h_{Att}
1·1	0·2750	0·250	0·8807	0·1908	0·2422	0·0525	0·2562	0·580	0·667	0·998	0·314	0·667
1·2	0·2988	0·225	0·8800	0·1904	0·2629	0·0569	0·2792					
1·3	0·3200	0·200	0·8840	0·1981	0·2829	0·0634	0·2939	0·570		0·970		
1·4	0·3388	0·175	0·8874	0·2076	0·3006	0·0703	0·3074					
1·5	0·3550	0·150	0·8910	0·2186	0·3163	0·0776	0·3193	0·549	0·659	0·906	0·284	0·636
1·7	0·3800	0·100	0·8991	0·2439	0·3417	0·0927	0·3384	0·518		0·820		
1·9	0·3950	0·050	0·9114	0·2775	0·3600	0·1096	0·3511	0·485	0·619	0·726	0·228	0·575
2·1	0·4	0	0·9326	0·3216	0·3731	0·1286	0·3573	0·451		0·628		
2·3	0·4	0	0·9604	0·3749	0·3842	0·1500	0·3659	0·427	0·581	0·543	0·170	0·485
2·5	0·4	0	0·9800	0·4205	0·3920	0·1682	0·3799	0·406		0·478		
2·7	0·4	0	0·9950	0·4624	0·3980	0·1850	0·3958	0·388	0·551	0·427	0·134	0·413
2·9	0·4	0	1·0072	0·5017	0·4029	0·2007	0·4123	0·373		0·386		
3·1	0·4	0	1·0175	0·5392	0·4070	0·2157	0·4290		0·531			0·359
3·3	0·4	0	1·0262	0·5750	0·4105	0·2300	0·4457	0·348		0·323	0·101	
3·5	0·4	0	1·0339	0·6096	0·4136	0·2438	0·4622					
3·7	0·4	0	1·0407	0·6427	0·4163	0·2571	0·4784	0·329	0·509	0·278	0·087	0·301

TABLE 3 (*a*)

Solutions for the Family of Plan-forms III, Fig. 4, at Incidence 15·3 deg

c	s	s'	η	ζ	y_0	z_0	Γ/U	C_L	h	A	$C_{L\,\mathrm{Att}}$	h_{Att}
0·400	0·2489	0·5778	0·9110	0·0974	0·2267	0·0243	0·2756					
0·425	0·2633	0·5722	0·9143	0·1037	0·2407	0·0273	0·2790					
0·450	0·2775	0·5667	0·9136	0·1048	0·2535	0·0291	0·2953					
0·500	0·3056	0·5556	0·9124	0·1071	0·2788	0·0327	0·3270					
0·600	0·3600	0·5333	0·9106	0·1113	0·3278	0·0401	0·3885	1·499		2·314	0·971	
0·800	0·4622	0·4889	0·9082	0·1192	0·4197	0·0551	0·5027					
1·000	0·5556	0·4444	0·9069	0·1272	0·5039	0·0707	0·6045					
1·200	0·6400	0·4000	0·9060	0·1357	0·5798	0·0868	0·6969					
1·400	0·7156	0·3556	0·9055	0·1453	0·6479	0·1040	0·7788	1·304	0·634	1·873	0·785	0·613
1·800	0·8400	0·2667	0·9048	0·1668	0·7601	0·1401	0·9191					
2·200	0·9289	0·1778	0·9109	0·1961	0·8461	0·1822	1·0058	1·084		1·416		
2·600	0·9822	0·0889	0·9195	0·2313	0·9032	0·2271	1·0692					
3·000	1·0	0	0·9386	0·2699	0·9386	0·2699	1·0850	0·873	0·535	1·000	0·419	0·467
3·400	1·0	0	0·9711	0·3315	0·9711	0·3315	1·1163					
3·800	1·0	0	0·9918	0·3772	0·9918	0·3772	1·1639	0·757		0·714		
4·200	1·0	0	1·0066	0·4217	1·0066	0·4217	1·2243					
4·600	1·0	0	1·0183	0·4649	1·0183	0·4649	1·2889	0·681	0·488	0·556	0·233	0·305
5·000	1·0	0	1·0278	0·5059	1·0278	0·5059	1·3534					
5·400	1·0	0	1·0364	0·5494	1·0364	0·5494	1·4303	0·636		0·455		
5·800	1·0	0	1·0440	0·5904	1·0440	0·5904	1·4921					
6·200	1·0	0	1·0503	0·6266	1·0503	0·6266	1·5524	0·595	0·467	0·385	0·161	0·226

TABLE 3 (*b*)

Solutions for the Family of Plan-forms III, Fig. 4, at Incidence 30·6 deg

c	s	s'	η	ζ	y_0	z_0	Γ/U	C_L	h	A	$C_{L\,\mathrm{Att}}$	h_{Att}
0·400	0·2489	0·5778	0·8800	0·1900	0·2190	0·0473	0·6204					
0·410	0·2547	0·5756	0·8817	0·1933	0·2245	0·0492	0·6296					
0·425	0·2633	0·5722	0·8835	0·1972	0·2326	0·0519	0·6461					
0·450	0·2775	0·5667	0·8853	0·2021	0·2457	0·0561	0·6762					
0·500	0·3056	0·5556	0·8856	0·2086	0·2706	0·0637	0·7455					
0·600	0·3600	0·5333	0·8819	0·2172	0·3175	0·0782	0·8959	3·755		2·314	1·943	
0·800	0·4622	0·4889	0·8798	0·2340	0·4067	0·1082	1·1701					
1·000	0·5556	0·4444	0·8777	0·2393	0·4876	0·1330	1·4218					
1·200	0·6400	0·4000	0·8843	0·2617	0·5660	0·1675	1·6255					
1·400	0·7156	0·3556	0·8824	0·2768	0·6314	0·1981	1·8530	3·365	0·635	1·873	1·571	0·613
1·800	0·8400	0·2667	0·8824	0·3241	0·7412	0·2723	2·2743					
2·200	0·9289	0·1778	0·8922	0·3655	0·8288	0·3395	2·5577	2·923		1·416		
2·600	0·9822	0·0889	0·9095	0·4193	0·8934	0·4119	2·7882					
3·000	1·0	0	0·9358	0·4872	0·9358	0·4872	2·9535	2·481	0·560	1·000	0·839	0·467
3·400	1·0	0	0·9755	0·5770	0·9755	0·5770	3·1347					
3·800	1·0	0	1·0017	0·6516	1·0017	0·6516	3·3335	2·240		0·714		
4·200	1·0	0	1·0208	0·7175	1·0208	0·7175	3·5316					
4·600	1·0	0	1·0356	0·7800	1·0356	0·7800	3·7363	2·050	0·497	0·556	0·466	0·305
5·000	1·0	0	1·0474	0·8378	1·0474	0·8378	3·9319					
5·400	1·0	0	1·0566	0·8845	1·0566	0·8845	4·0948	1·892		0·455		
5·800	1·0	0	1·0647	0·9301	1·0647	0·9301	4·2591					
6·200	1·0	0	1·0719	0·9783	1·0719	0·9783	4·4339	1·769	0·468	0·385	0·323	0·226

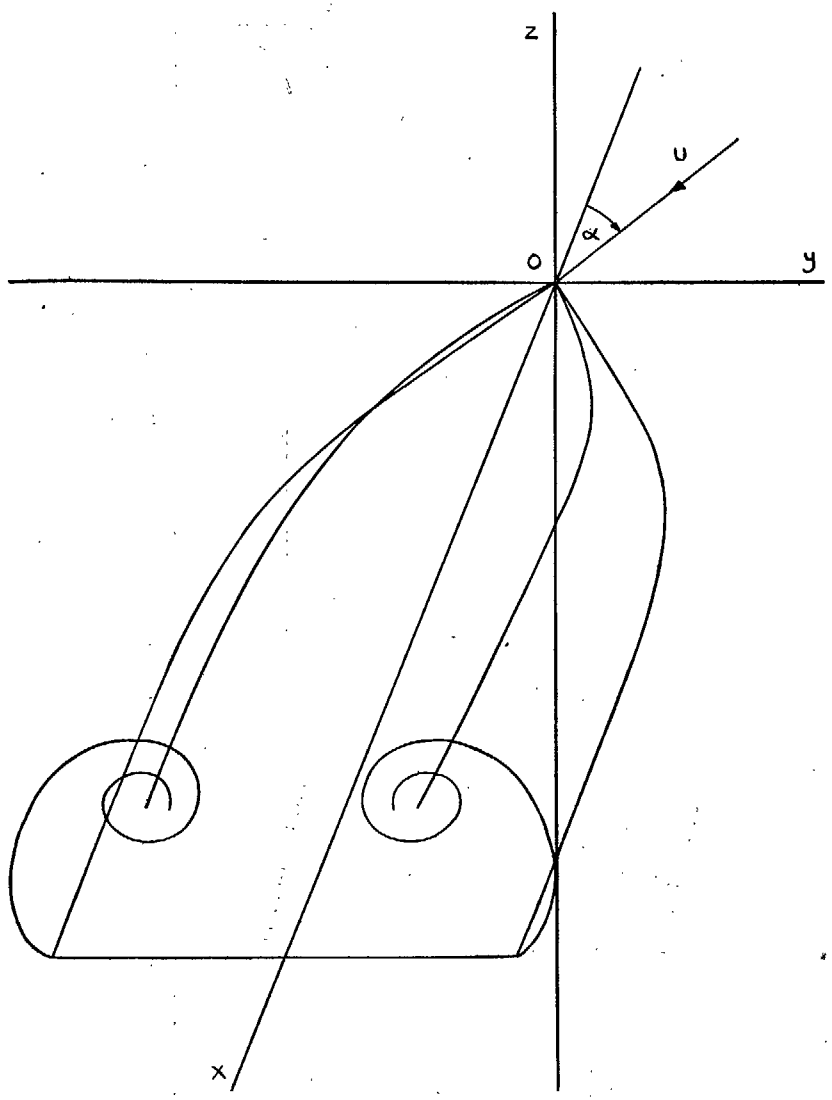

FIG. 1. Co-ordinate system.

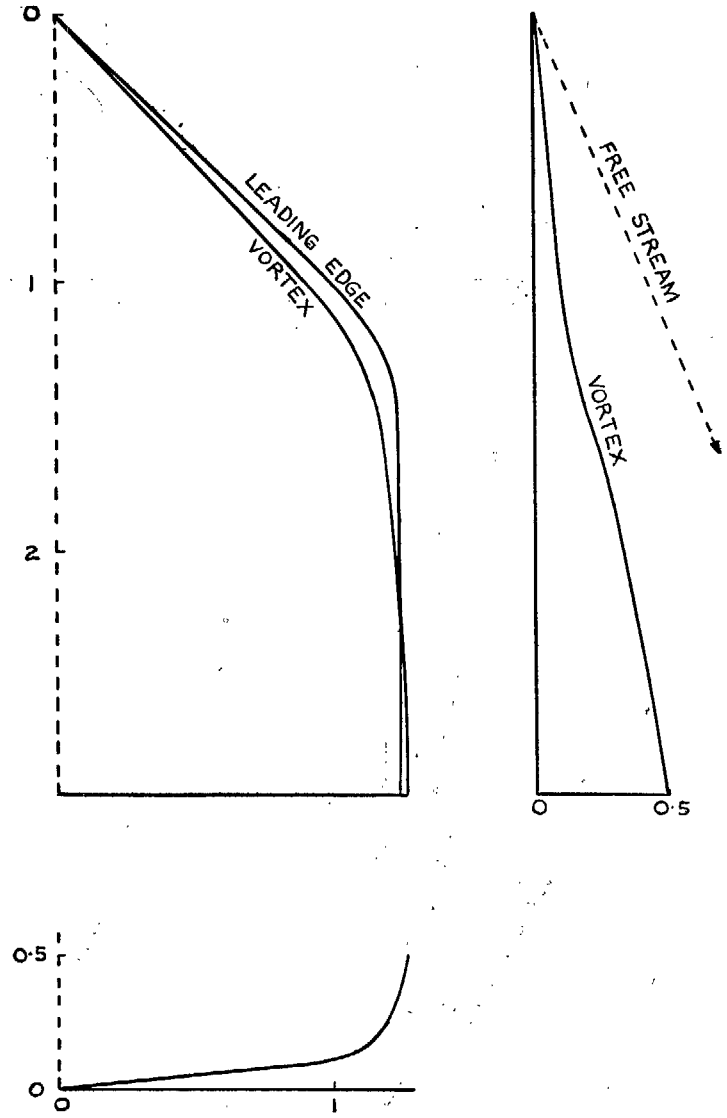

FIG. 2. Three projections of plan-form family I at $\alpha = 22{\cdot}9$ deg.

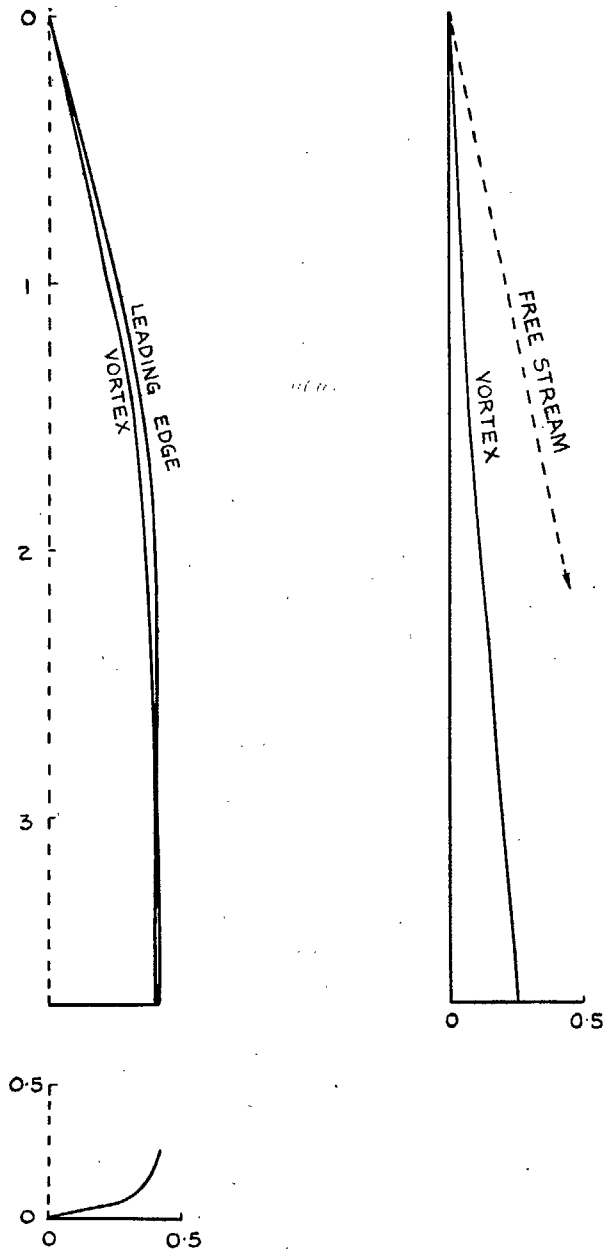

FIG. 3. Three projections of plan-form family II at $\alpha = 11{\cdot}45$ deg.

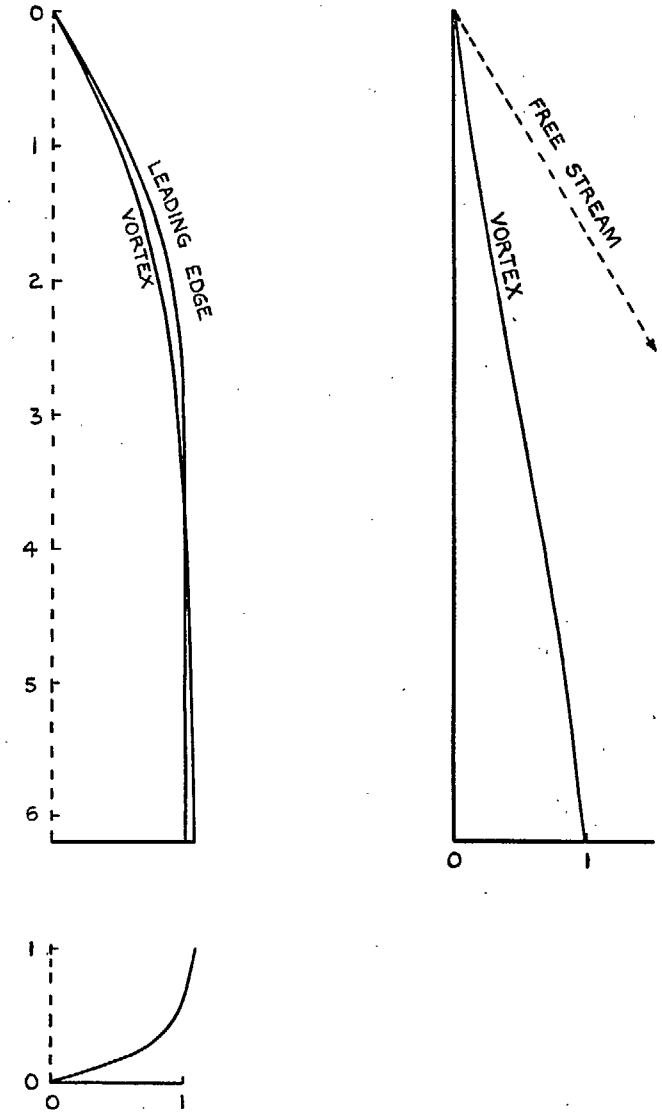

FIG. 4. Three projections of plan-form family III at $\alpha = 30{\cdot}6$ deg.

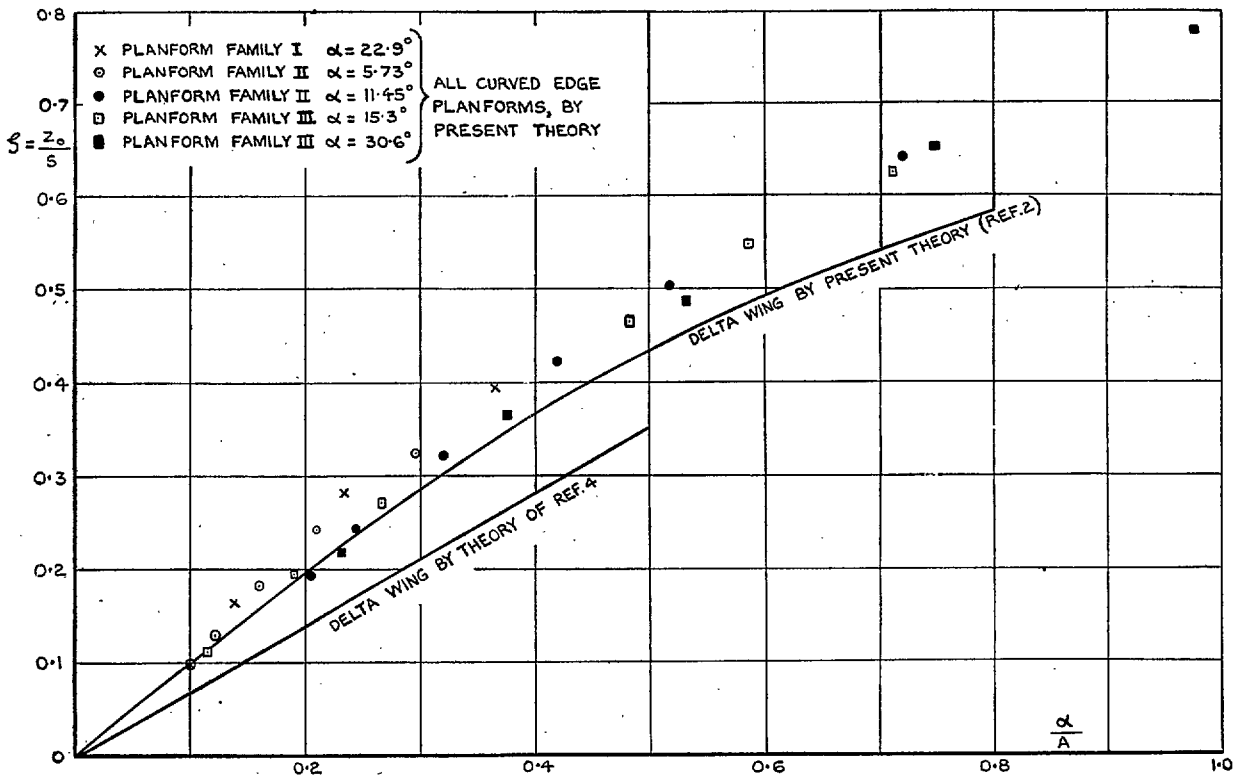

FIG. 5. Theoretical variation of the height of the vortex above the wing trailing edge.

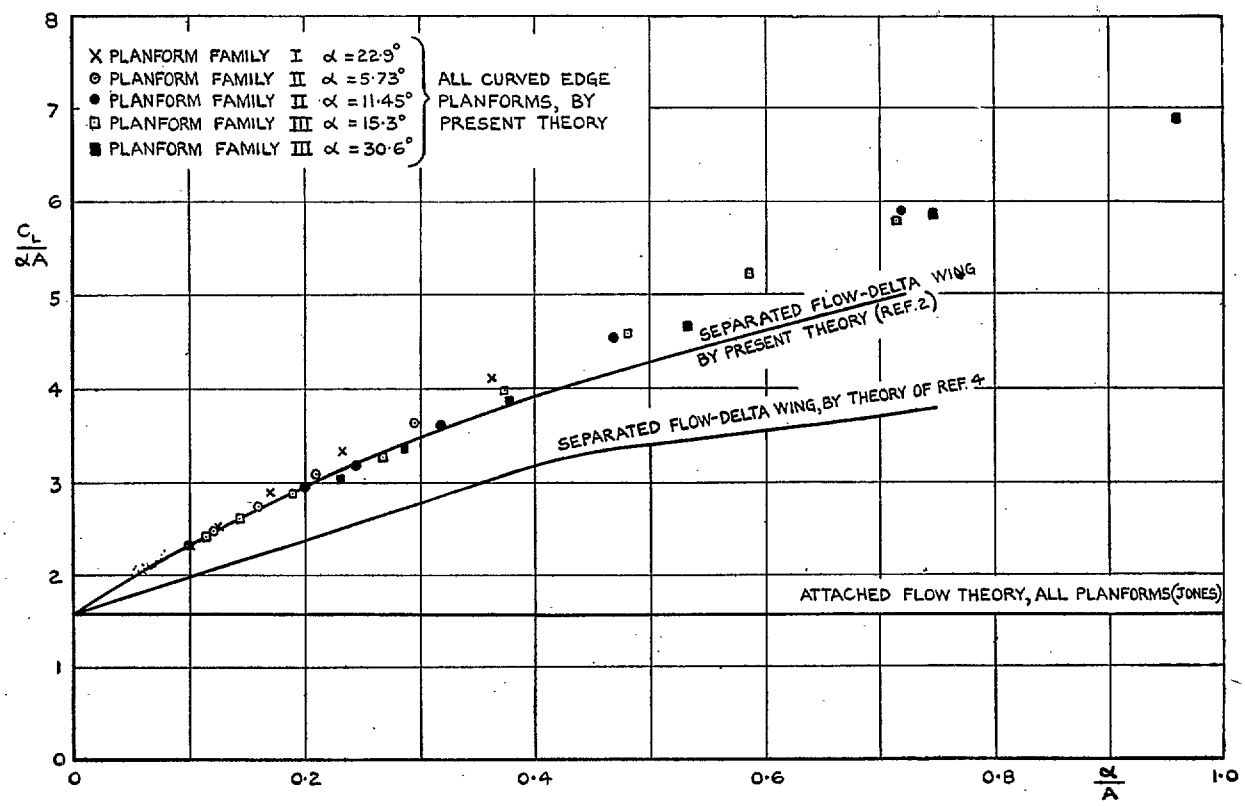

FIG. 6. Theoretical variation of the normal-force coefficient.

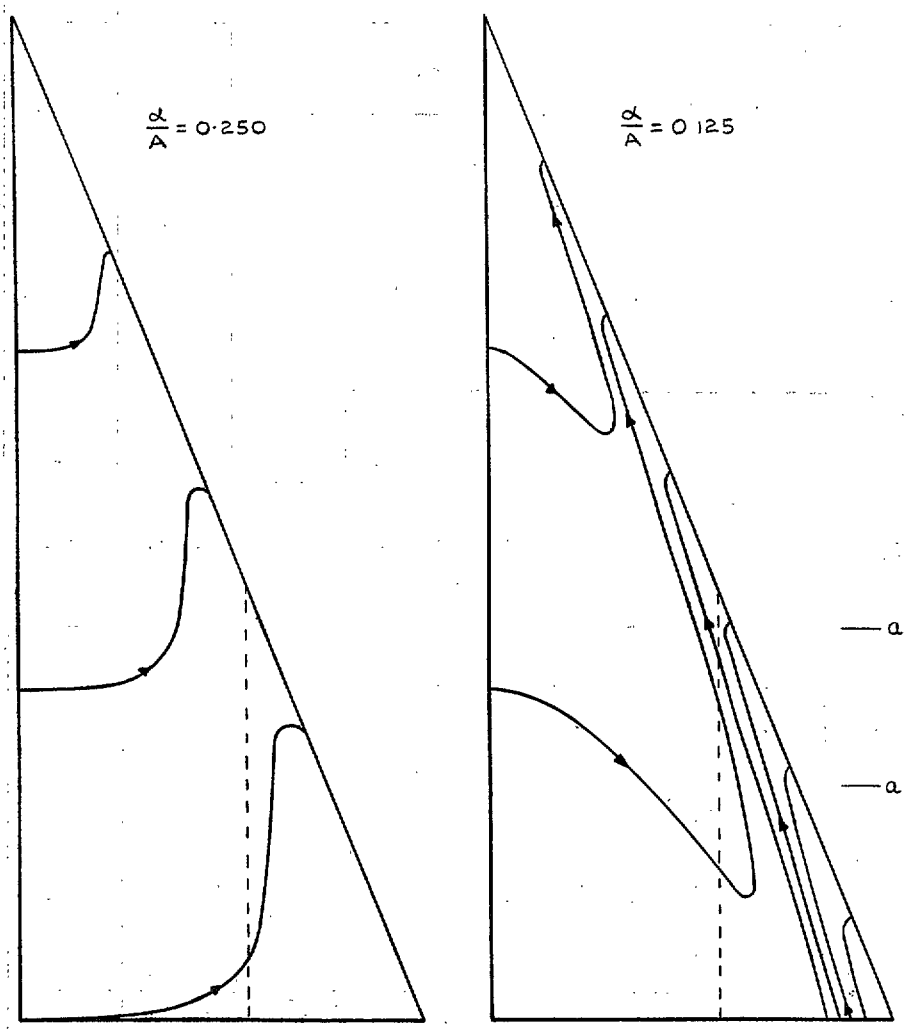

FIG. 7. Bound vortices on a delta wing for $\alpha/A = 0{\cdot}25, 0{\cdot}125$.

(74986) Wt. 53/2293 K. 7 7/59 Hw.

PRINTED IN GREAT BRITAIN

Publications of the Aeronautical Research Council

ANNUAL TECHNICAL REPORTS OF THE AERONAUTICAL RESEARCH COUNCIL (BOUND VOLUMES)

1939 Vol. I. Aerodynamics General, Performance, Airscrews, Engines. 50*s.* (52*s.*).
Vol. II. Stability and Control, Flutter and Vibration, Instruments, Structures, Seaplanes, etc. 63*s.* (65*s.*)

1940 Aero and Hydrodynamics, Aerofoils, Airscrews, Engines, Flutter, Icing, Stability and Control, Structures, and a miscellaneous section. 50*s.* (52*s.*)

1941 Aero and Hydrodynamics, Aerofoils, Airscrews, Engines, Flutter, Stability and Control, Structures. 63*s.* (65*s.*)

1942 Vol. I. Aero and Hydrodynamics, Aerofoils, Airscrews, Engines. 75*s.* (77*s.*)
Vol. II. Noise, Parachutes, Stability and Control, Structures, Vibration, Wind Tunnels. 47*s.* 6*d.* (49*s.* 6*d.*)

1943 Vol. I. Aerodynamics, Aerofoils, Airscrews. 80*s.* (82*s.*)
Vol. II. Engines, Flutter, Materials, Parachutes, Performance, Stability and Control, Structures. 90*s.* (92*s.* 9*d.*)

1944 Vol. I. Aero and Hydrodynamics, Aerofoils, Aircraft, Airscrews, Controls. 84*s.* (86*s.* 6*d.*)
Vol. II. Flutter and Vibration, Materials, Miscellaneous, Navigation, Parachutes, Performance, Plates and Panels, Stability, Structures, Test Equipment, Wind Tunnels. 84*s.* (86*s.* 6*d.*)

1945 Vol. I. Aero and Hydrodynamics, Aerofoils. 130*s.* (132*s.* 9*d.*)
Vol. II. Aircraft, Airscrews, Controls. 130*s.* (132*s.* 9*d.*)
Vol. III. Flutter and Vibration, Instruments, Miscellaneous, Parachutes, Plates and Panels, Propulsion. 130*s.* (132*s.* 6*d.*)
Vol. IV. Stability, Structures, Wind Tunnels, Wind Tunnel Technique. 130*s.* (132*s.* 6*d.*)

Annual Reports of the Aeronautical Research Council—

1937 2*s.* (2*s.* 2*d.*) 1938 1*s.* 6*d.* (1*s.* 8*d.*) 1939–48 3*s.* (3*s.* 5*d.*)

Index to all Reports and Memoranda published in the Annual Technical Reports, and separately—

April, 1950 - - - - R. & M. 2600 2*s.* 6*d.* (2*s.* 10*d.*)

Author Index to all Reports and Memoranda of the Aeronautical Research Council—

1909—January, 1954 R. & M. No. 2570 15*s.* (15*s.* 8*d.*)

Indexes to the Technical Reports of the Aeronautical Research Council—

December 1, 1936—June 30, 1939	R. & M. No. 1850	1*s.* 3*d.* (1*s.* 5*d.*)
July 1, 1939—June 30, 1945	R. & M. No. 1950	1*s.* (1*s.* 2*d.*)
July 1, 1945—June 30, 1946	R. & M. No. 2050	1*s.* (1*s.* 2*d.*)
July 1, 1946—December 31, 1946	R. & M. No. 2150	1*s.* 3*d.* (1*s.* 5*d.*)
January 1, 1947—June 30, 1947	R. & M. No. 2250	1*s.* 3*d.* (1*s.* 5*d.*)

Published Reports and Memoranda of the Aeronautical Research Council—

Between Nos. 2251–2349	R. & M. No. 2350	1*s.* 9*d.* (1*s.* 11*d.*)
Between Nos. 2351–2449	R. & M. No. 2450	2*s.* (2*s.* 2*d.*)
Between Nos. 2451–2549	R. & M. No. 2550	2*s.* 6*d.* (2*s.* 10*d.*)
Between Nos. 2551–2649	R. & M. No. 2650	2*s.* 6*d.* (2*s.* 10*d.*)
Between Nos. 2651–2749	R. & M. No. 2750	2*s.* 6*d.* (2*s.* 10*d.*)

Prices in brackets include postage

HER MAJESTY'S STATIONERY OFFICE

York House, Kingsway, London W.C.2; 423 Oxford Street, London W.1; 13a Castle Street, Edinburgh 2; 39 King Street, Manchester 2; 2 Edmund Street, Birmingham 3; 109 St. Mary Street, Cardiff; Tower Lane, Bristol 1; 80 Chichester Street, Belfast, *or through any bookseller.*

S.O. Code No. 23-3116